



Undrained Monotonic Compression, Cyclic Triaxial and Cyclic Simple Shear Response of Natural Soils: Strength and Excess Pore Water Pressure Response

Majid Hussain¹ (✉)  and Ajanta Sachan² 

¹ Department of Civil Engineering, NIT Srinagar, Srinagar, India
majid.h@nitsri.ac.in

² Civil Engineering, IIT Gandhinagar, Gandhinagar, India

Abstract. The mechanical response of soils is governed by several factors including loading and boundary conditions. Under undrained boundary conditions, the nature and magnitude of excess pore water pressure (PWP) control the evolution of effective confining pressure (p') which in turn controls the evolution of shear stress. In this study, we investigate the shear strength and excess PWP response of natural soils under monotonic triaxial compression (TX), cyclic triaxial (CTX) and cyclic simple shear (CSS) testing conditions. The experimental study consisted of evaluating the undrained response of 31 natural soils collected from 10 locations (including 5 dams) in the Kutch region of India. The significance of the investigation lies in the fact that the region is seismically active with a proven history of devastating earthquakes. The most recent earthquake, the 2001 Bhuj earthquake, created large scale destruction with incidences of widespread earthquake liquefaction. The experimental investigation revealed that the undrained response of the soils at the in-situ density is controlled by both the fines content (FC) and plasticity index (PI). For cohesionless soils, FC governed the soil behaviour whereas for cohesive soils PI dominated the soil behaviour. Cohesionless soils exhibited intense strain softening (SS) under monotonic triaxial compression whereas cohesive soils displayed limited strain softening (LSS). Under CTX and CSS testing conditions, cohesionless soils exhibited very low liquefaction resistance (less than 10 cycles) whereas cohesive soils did not liquefy in 50 cycles. However, cohesive soils did exhibit significant degradation in cyclic strength, which was controlled by PI. The excess PWP was found to be contractive for all three conditions. For cyclic loading, PWP was found to be 30% higher for CSS conditions compared to the CTX conditions. Cyclic simple shear simulates the earthquake conditions better and should be considered for seismic and liquefaction analysis.

Keywords: Liquefaction · Cyclic triaxial · Cyclic simple shear · Earthquake · Excess pore water pressure

1 Introduction

Soil behavior is governed by several factors including nature and type of loading, boundary conditions and soil properties [1, 2]. Soil behavior under static and dynamic loading

has been explored by many researchers [3–5]. The effect of strain rate, relative density and fines content on the soil behavior has been explored. Increased stiffness, increased peak shear strength and reduced strain at peak shear strength were observed with increased strain rate [6]. The influence of loading history on the undrained cyclic response of granular soils was explored under both the isotropic and anisotropic conditions [7, 8]. Soil behavior under cyclic loading is affected by characteristics of the input loading such as stress amplitude (γ), frequency (f) and the number of loading cycles (N) [9–12]. Loading under undrained conditions static as well as cyclic may lead to static and cyclic liquefaction respectively. This is characterized by lower mobilized shear strength and large excess pore water pressure. Fewer incidences of static liquefaction (Nerleck Berm, Aberfan Landslide, Merriespruit tailings dam failure) as compared to cyclic liquefaction are documented [13]. In the knowledge of the authors, very few studies have explored the link between static and cyclic liquefaction [14]. In these studies, a strong correlation between the state of the stress at the onset of instability under static and cyclic loading has been observed. The impending cyclic liquefaction could very well be predicted from the monotonic response. In this study, undrained soil behavior under monotonic triaxial compression, cyclic triaxial and cyclic simple shear conditions from the perspective of shear strength and excess pore water pressure is studied. Soil behavior of 31 natural soils from Kutch, a region in western India is investigated. Hussain and Sachan [15] investigated the link between the conditions triggering the static and cyclic liquefaction for a typical silty-sand of the region. The results were found to be in agreement with the those reported by [14].

2 Materials and Methods

In this study, 32 disturbed representative soil specimens were collected from 10 locations, including 5 major dams, at depths ranging from 0.5 m to 2.5 m from the Kutch region (Fig. 1). The locations were primarily selected on the basis of evidence of earthquake liquefaction during the 2001 Bhuj earthquake. During this seismic event, widespread liquefaction over an extent of greater than 15,000 m² was observed, thereby aggravating the earthquake damage. The basic geotechnical properties of the soils of the region can be found elsewhere [15] and are presented in Table 1. The soils in the region are mostly sandy soils with fines content varying from 11% to 83%. The in-situ dry density of the soils, in the present investigation, varied from 13.37 kN/m³ to 17.71 kN/m³. The plasticity index of the soils varied from non-plastic to 23%. From the total of 32 soil samples, 17 classified as silty-sands, 9 as clayey sands, 1 as low plasticity silt, 3 as clay with low plasticity, and 2 clay with high plasticity. Thus the soils explored in the current study, represent natural soil deposits with varying characteristics including in-situ density, particle characteristics (size, shape and texture), fines content, nature of fines and plasticity index.

Three series of tests including isotropically consolidated undrained compression triaxial (TX) tests, isotropically consolidated undrained cyclic triaxial (CTX) tests, constant volume cyclic simple shear (CSS) tests were performed on the 31 soil samples. The specimens for the three series of tests were prepared by the moist tamping technique at the in-situ density and moisture content. The specimens for TX and CTX were consolidated to an effective confining pressure of 100 kPa and then subjected to monotonic

Table 1. (continued)

Soil name	Depth m	γ_{di} kN/m ³	G_s	GSD				FC %	Atterberg limits			Soil class
				G	S	M	C		LL	PL	PI	
				%	%	%	%		%	%	%	
<i>Chobari</i>		23°30.722' N		70°20.881' E								
S13	0.5	17.51	2.70	0	56	42	2	44	24.2	14.2	10.0	SC
S14	1.5	16.96	2.71	0	51	42	7	49	26.2	14.8	11.4	SC
S15	2.5	17.57	2.70	0	59	37	4	41	24.6	16.2	8.4	SC
<i>Khadir</i>		23°50.82' N		70°14.39' E								
S16	0.5	15.94	2.66	2	79	17	2	19	16.9	NP	NP	SM
S17	1.5	16.82	2.66	1	74	22	3	25	15.6	NP	NP	SM
S18	2.5	16.96	2.66	2	88	9	1	10	13.7	NP	NP	SP-SM
<i>Tappar Dam</i>		23°15.017' N		70°07.586' E								
S19	0.5	17.36	2.67	0	58	24	18	42	34.1	11.2	22.9	SC
S20	1.5	16.39	2.66	5	66	14	15	29	31.4	10.1	21.3	SC
S21	2.5	17.67	2.68	4	72	14	10	24	22.2	10.5	11.7	SC
<i>Budharmora</i>		23°20.634' N		70°11.501' E								
S22	0.5	17.71	2.68	2	69	21	8	29	23.2	14.6	8.6	SC
S23	1.5	14.27	2.71	1	34	46	19	65	44.3	15.7	28.6	CL
S24	2.5	12.26	2.70	2	18	57	23	80	65.8	26.9	38.9	CH
<i>Banniari</i>		23°24.299' N		70°09.910' E								
S25	0.5	13.37	2.74	0	17	81	2	83	26.4	NP	NP	ML
S26	1.5	14.59	2.75	0	5	68	27	95	47.2	18.6	28.6	CL
S27	2.0	16.26	2.68	0	68	26	6	32	24.6	11.6	13.0	SC
S28	2.5	17.60	2.69	1	78	13	8	21	28.0	11.7	16.3	SC
<i>Shivlakha Dam</i>		23°24.659' N		70°35.128' E								
S29	0.5	14.43	2.69	0	71	25	4	29	16.8	NP	NP	SM
S30	1.5	14.88	2.70	1	88	9	2	11	17.4	NP	NP	SP-SM
S31	2.0	16.37	2.69	1	74	18	7	25	15.0	NP	NP	SM
S32	2.5	13.40	2.68	0	28	50	22	72	39.0	15.5	23.5	CL

compression and axial cyclic loading respectively. Specimens for CSS were consolidated to vertical effective stress of 100 kPa under K_0 conditions and subjected to horizontal cyclic loading. The details of the experimental programme for TX, CTX and CSS tests can be found elsewhere [16–18]. Specimen S1 was not included in any of the test series whereas specimens S10, S28, and S32 were not included in the CTX and CSS test series.

These samples could not be tested as they could not be saturated due to the presence of large amount of high plasticity fines. Soils samples S1 and L2 were collected from very close locations and had similar properties.

2.1 Loading Conditions

The loading conditions for three series of tests were different. For the CIUC tests, the nature of the loading was static whereas for CTX and CSS the loading was cyclic in nature. The shearing of the specimens for all three series was deformation controlled. The deformation rate for CIUC tests was 0.1 mm/min, for CTX and CSS tests the frequency of cyclic loading was the same 0.1 Hz, however, the deformation amplitude was 0.4 mm and 0.12 mm respectively resulting in the strain amplitude of 0.6 % for both series of the tests. Figure 2 shows the pictorial representation of the loading for the three conditions along with the specimen size.

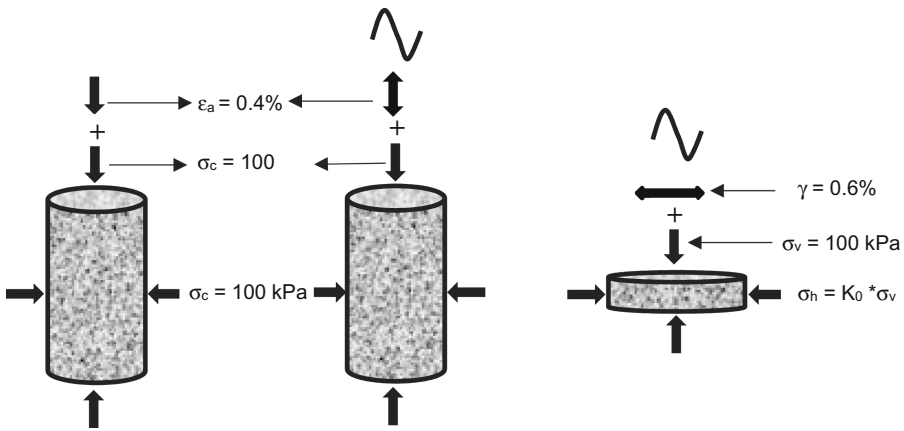


Fig. 2. Loading conditions and specimens size for the three series (a) CIUC, (b) CTX and (c) CSS.

3 Results and Discussion

The strength and excess pore pressure response of the Kutch soils as observed from the carefully conducted experiments including three series CIUC triaxial, CTX, and CSS tests are analyzed. The results are generalized for typical silty-sand and clayey-sand behaviour under the three loading conditions. The effect of fines content and plasticity index on the observed behavior is discussed.

3.1 Response Under CIUC Conditions

Figure 3 shows the stress-strain and pore pressure response of a typical silty-sand (S2) from the Kutch region under monotonic compression (CIUC) loading. The specimen

mobilized deviatoric stress (σ_d) rapidly and attained peak value at axial strain (ϵ_p) value of 0.47%. After attaining the peak value, intense strain-softening behavior was observed. The specimen displayed a very low deviatoric stress value at large strains (residual strength) (Fig. 3a). The specimen developed rapid and large excess pore pressure (u) response in agreement with the stress-strain response (Fig. 3a). The intense strain-softening could be attributed to the extremely large pore pressure values which nearly reached to initial effective confining pressure (p'_i) of 100 kPa. Figure 4 shows the effective stress path (ESP) response of the typical silty-sand (S2) from the Kutch region. The ESP captures the signature of both the stress-strain and pore pressure response. Right from the onset of shearing, the effective confining pressure (p') reduced and attained very low values. The stress-path after attaining peak deviatoric stress (σ_{dp}) moved towards the stress origin and mobilized very low shear strength nearly manifesting static liquefaction. Similar behavior was displayed by the remaining silty-sands. However, σ_{dp} , rate of development of excess pore water pressure, and residual strength (σ_{dr}) was significantly affected by the amount of FC and PI (Table 2).

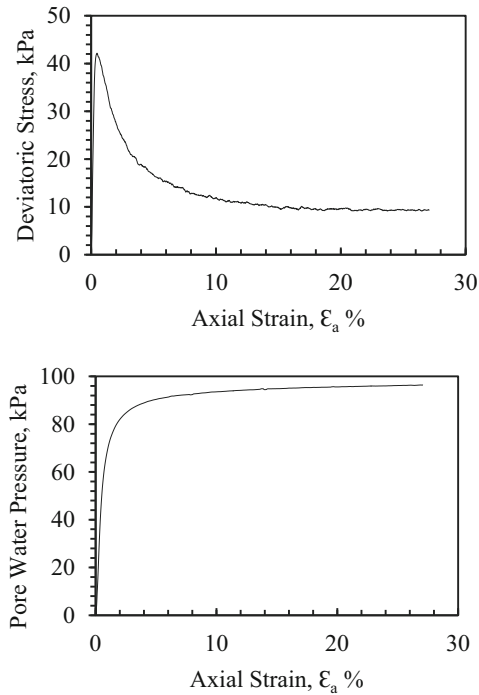


Fig. 3. Behavior of typical silty-sand (S2) under CIUC conditions. (a) Stress-strain and (b) Excess pore pressure

Table 2. Summary of CIUC triaxial tests. Parameters at peak deviatoric stress, and large strains

Soil name	M (%)	C (%)	FC (%)	σ_{dp}	ϵ_p	u_p	σ_{dr}	ϵ_r	u_r
<i>Chang Dam</i>									
S2	15	3	18	42	0.45	46	9.3	25	96
S3	17	2	19	38	0.42	48	4.6	25	96
<i>Kharoi</i>									
S4	13	5	18	34	0.6	57	16	25	92
S5	9	2	11	40	0.5	53	13	25	96
S6	11	2	13	42	0.48	52	9.2	25	98
<i>Suvai Dam</i>									
S7	21	7	28	38	0.54	51	14	23	95
S8	19	5	24	38	0.48	49	18	22	89
S9	14	3	17	36	0.42	45	5	25	97
<i>Fatehgarh Dam</i>									
S10	62	37	99	–	–	–	–	–	–
S11	42	3	45	44	0.55	51	18	25	95
S12	21	1	22	67	0.56	46	1.2	19	95
<i>Chobari</i>									
S13	42	2	44	48	0.76	53	42	25	85
S14	42	7	49	49	0.5	34	52	25	75
S15	37	4	41	37	0.5	28	47	25	76
<i>Khadir</i>									
S16	17	2	19	33	0.46	50	5.8	25	96
S17	22	3	25	38	0.54	53	13	25	93
S18	9	1	10	42	0.38	44	29	25	90
<i>Tappar Dam</i>									
S19	24	18	42	45	0.5	35	60	25	73
S20	14	15	29	49	0.5	41	54	25	72
S21	14	10	24	49	0.5	41	53	25	80
<i>Budharmora</i>									
S22	21	8	29	46	0.5	44	29	25	90
S23	46	19	65	27	0.5	20	72	25	76
S24	57	23	80	31	0.5	15	61	25	66
<i>Banniari</i>									

(continued)

Table 2. (continued)

Soil name	M (%)	C (%)	FC (%)	σ_{dp}	ϵ_p	u_p	σ_{dr}	ϵ_r	u_r
S25	81	2	83	49	0.56	46	6	25	97
S26	68	27	95	37	0.5	21	77	25	70
S27	26	6	32	45	0.76	52	43	25	85
S28	13	8	21	42	0.7	46	37	25	85
<i>Shivlakha Dam</i>									
S29	25	4	29	40	0.47	44	8	25	96
S30	9	2	11	53	0.45	48	5.6	25	98
S31	18	7	25	50	0.5	37	7.6	25	96
S32	50	22	72	38	0.5	30	50	25	75

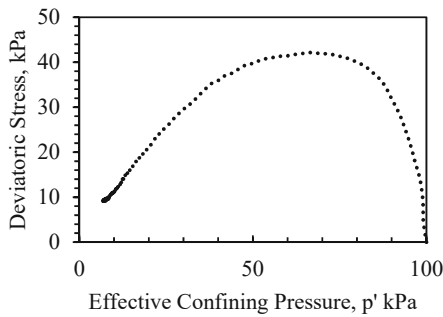


Fig. 4. Effective stress path (ESP) response of typical silty-sand (S2)

Figure 5 shows the stress-strain and pore pressure response of a typical clayey-sand (S19) of the Kutch region. It is evident that the response depicted by S19 is significantly different from the S2. Specimen S19 mobilized higher deviatoric stress as compared to S19 and did not show any strain softening. The mobilized deviatoric stress continued to increase slowly (Fig. 5b).

Specimen S19 exhibited gradual development of pore water pressure and reached a value of 73 kPa, significantly lower as compared to S2. The presence of higher and plastic fines led to the behavior observed in S19. Figure 6 shows the ESP response of S19. After an initial decrease, p' increased displaying strain hardening behavior. This could be attributed to the nature of fines. While S11 was non-plastic (silty-sand), the nature of fines was plastic in case of S19. Specimen S11 and S19 had nearly same FC (Table 2). However, the response of the two specimens was observed to be significantly different (Figs. 5 and 6).

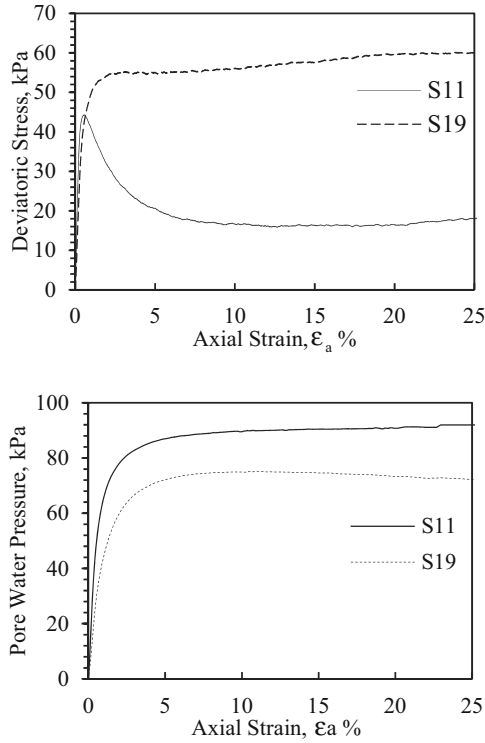


Fig. 5. Behavior of typical silty-sand (S19) and silty-sand (S11) under CIUC conditions. (a) Stress-strain and (b) Excess pore water pressure

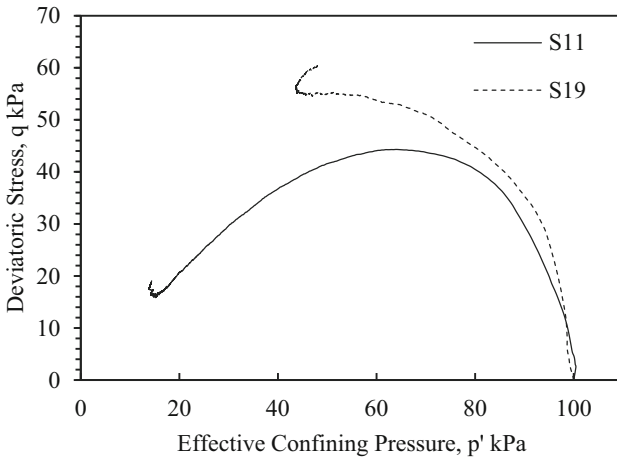


Fig. 6. Effective stress path (ESP) response of typical clayey-sand (S19) and silty-sand (S11)

3.2 Response Under CTX Conditions

Figure 7 shows the response of a typical silty-sand specimen S2 subjected to CTX loading after isotropic consolidation at 100 kPa. The observations reveal that after four loading cycles the hysteresis loops flattened and mobilized very low cyclic stresses (Fig. 7a) while large pore pressures developed rapidly (Fig. 7a). Large and rapid pore pressure developed leading to reduced mean effective pressures which subsequently led to very low cyclic stresses at constant strain. After four loading cycles, pore pressure ratio ($r_u = \frac{\text{excess pore water pressure}, \Delta u}{\text{initial effective confg pressure}, p_i}$) attained values nearly equal to unity signifying initial liquefaction (Fig. 7b). Figure 8 shows the effective stress of the specimen S2 subject CTX loading. It is evident that after four cycles of loading mean effective confining pressure reduced nearly to zero. At reduced p' , the specimen exhibited very low cyclic resistance leading to liquefaction. The cyclic stress ratio ($CSR = \frac{\sigma_d}{p'_i}$) at the end of the 5th cycle was observed to be very low, 0.03, signifying σ_d of 3 kPa (Table 3). Soils classified as silty-sand showed similar behavior with large and rapid generation of Δu leading to huge reduction in p' . Reduced p' values mean lower shear strength for cohesionless soils which is evident from the stress-strain response of the silty-sand specimens. With reduced mobilized shear strength (σ_d), CSR values also decreased.

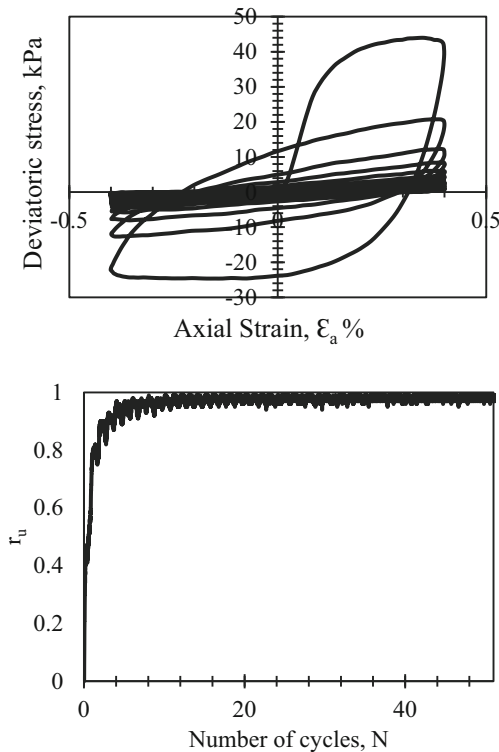


Fig. 7. Behavior of typical silty-sand (S11) under CTX conditions. (a) Stress-strain and (b) Excess pore water pressure

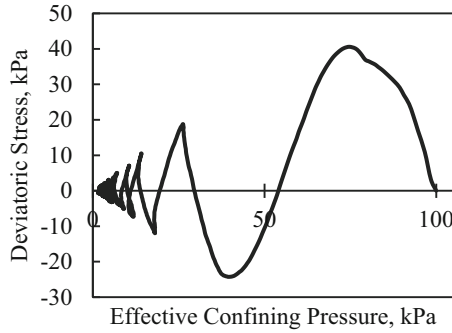


Fig. 8. Effective stress path (ESP) response of typical silty-sand (S11)

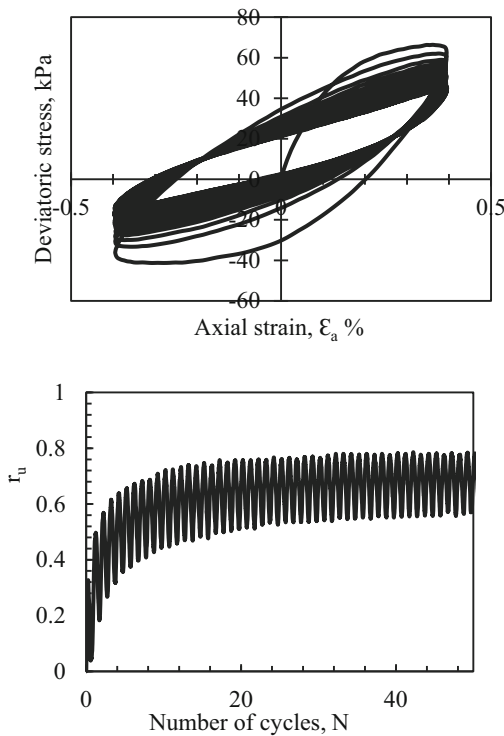


Fig. 9. Behavior of typical clayey-sand (S19) under CTX conditions. (a) Stress-strain and (b) Excess pore water pressure

Figure 9 shows the cyclic behavior of a typical clayey-sand (S19) of Kutch region. It is evident that the specimen exhibited higher resistance to cyclic loading as compared to S2. The presence of plastic fines resulted in mobilization of higher cyclic stresses as well as reduced and delayed excess pore water pressure. The hysteresis loops instead of flattening stabilized after five cycles (Fig. 9a). Excess pore pressure values also stabilized,

however, the difference between the minimum and maximum r_u was higher as compared to S2. Even after 50 cycles of loading the r_u value was observed to be 0.75. Figure 10 shows the evolution of effective stress path for specimen S19. It could be observed during the 50 cycles not much degradation in cyclic strength occurred and p' values did not go below 30 kPa which lead to specimen not liquefying in 50 cycles. After 5 loading cycles, CSR was observed to be 0.28 much higher as compared to S2 (0.03) (Table 3). Specimen S11 with similar fines content as that of S19 displayed significantly different behavior and liquefied in 27 cycles with CSR at the end of 5th cycle equal to 0.11. The results from the CTX tests are presented in Table 3. Silty-sands liquefied within 5 cycles whereas clayey-sand did not liquefy. The amount of fines as well as their nature controlled the cyclic behavior of Kutch soils.

Table 3. Summary of CTX tests

Soil name	FC (%)	Clay (%)	Peak parameters at the end of								Number of cycles to liquefaction, N_L
			1 st Cycle				5 th Cycle				
			σ_{dmax} (kPa)	p' (kPa)	Δu (kPa)	CSR	σ_{dmax} (kPa)	p' (kPa)	Δu (kPa)	CSR	
<i>Chang Dam</i>											
S2	18	3	44.8	27.0	75	0.22	6.6	9.0	96	0.03	4
S3	19	2	31.3	35.0	67	0.15	8.0	11.0	89	0.04	9
<i>Kharoi</i>											
S4	18	5	36.2	32.0	70	0.18	10.9	12.0	90	0.05	31
S5	11	2	43.2	27.0	79	0.21	5.7	9.0	96	0.03	4
S6	13	2	47.7	25.0	80	0.24	3.4	4.0	95	0.02	5
<i>Suvai Dam</i>											
S7	28	7	38.6	34.0	67	0.19	9.4	10.0	90	0.05	23
S8	24	5	35.3	42.0	69	0.17	9.8	15.0	90	0.05	18
S9	17	3	41.8	28.0	74	0.21	7.0	5.0	95	0.03	5
<i>Fatehgarh Dam</i>											
S11	45	3	43.8	46.0	59	0.22	21.1	20.0	84	0.11	27
S12	22	1	52.2	25.0	78	0.26	4.0	4.0	97	0.02	3
<i>Chobari</i>											
S13	44	2	58.1	44.0	61	0.29	29.1	20.0	82	0.15	>50
S14	49	7	46.7	86.0	16	0.23	21.9	67.0	35	0.11	>50
S15	41	4	47.7	68.0	35	0.24	12.0	42.0	60	0.06	>50
<i>Khadir</i>											

(continued)

Table 3. (continued)

Soil name	FC (%)	Clay (%)	Peak parameters at the end of								Number of cycles to liquefaction, N_L
			1 st Cycle				5 th Cycle				
			σ_{dmax} (kPa)	p' (kPa)	Δu (kPa)	CSR	σ_{dmax} (kPa)	p' (kPa)	Δu (kPa)	CSR	
S16	19	2	39.5	33.0	71	0.20	9.5	12.0	93	0.05	7
S17	25	3	41.7	26.0	76	0.21	7.4	4.0	97	0.04	5
S18	10	1	67.9	28.0	75	0.34	3.6	3.0	97	0.02	3
<i>Tappar Dam</i>											
S19	42	18	66.4	73.0	36	0.33	55.4	51.0	64	0.28	>50
S20	29	15	55.4	66.0	38	0.27	38.5	48.0	62	0.19	>50
S21	24	10	45.2	64.0	38	0.23	21.2	41.0	60	0.11	>50
<i>Budharmora</i>											
S22	29	8	51.7	58.0	44	0.26	20.1	11.0	87	0.1	10
<i>Banniari</i>											
S25	83	2	53.3	41.0	63	0.27	7.7	5.0	95	0.04	5
S26	32	6	39.3	60.0	42	0.20	18.0	31.0	71	0.09	>50
S27	21	8	45.1	53.0	36	0.27	23.6	24.0	80	0.12	>50
<i>Shivlakra Dam</i>											
S29	29	4	39.0	30.0	73	0.20	4.5	7.0	97	0.02	5
S30	11	2	59.6	32.0	72	0.29	4.0	5.0	96	0.02	5
S31	25	7	62.2	33.0	73	0.31	13.5	6.0	95	0.07	5

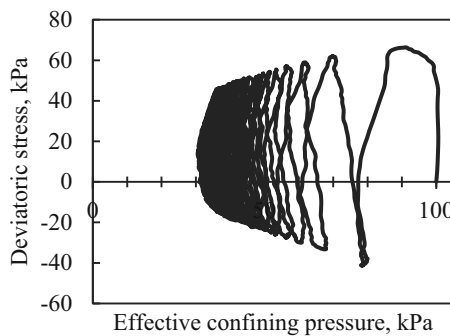


Fig. 10. Effective stress path (ESP) response of typical clayey-sand (S19)

3.3 Response Under CSS Conditions

Figure 11 shows the stress-strain and pore pressure response of a typical silty-sand (S2) of Kutch region. The hysteresis loop flattened after second cycle of loading indicating large and rapid reduction in cyclic resistance (Fig. 11a).

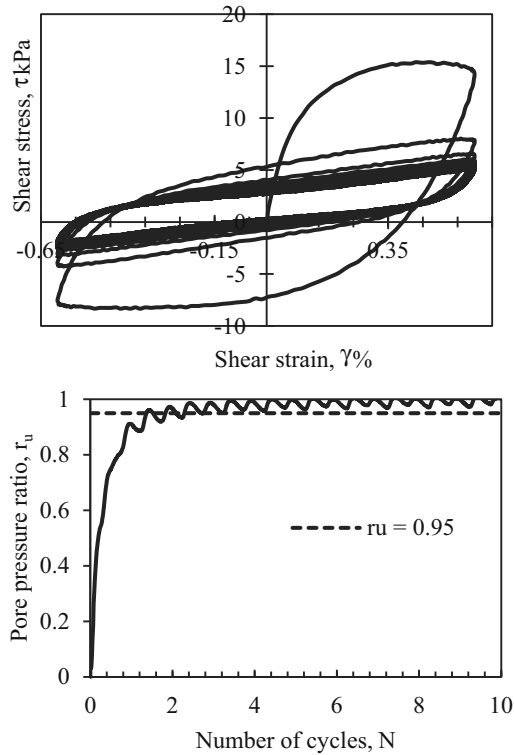


Fig. 11. Behavior of typical silty-sand (S2) under CSS conditions. (a) Stress-strain and (b) Excess pore water pressure

Shear stresses of magnitude 15.6 kPa were mobilized during the first cycle; much lower as compared to the deviatoric stress under the CTX conditions. Pore pressure ratio exceeded 0.95 just after two cycles of loading resulting to negligible confinement; a state of initial liquefaction (Fig. 11b). The specimen reached the state of initial liquefaction in two cycles.

Figure 12 shows the response of a typical clayey-sand (S19) of Kutch region. The hysteresis loops stabilized after a small reduction in mobilized shear stress (Fig. 12a). With further loading, the reduction in cyclic strength was lower and slower. Pore pressure ratio response also showed a similar trend (Fig. 12b). More than 50% (43 kPa) of the ultimate (80 kPa) pore water pressure developed during the first cycle. After the first loading cycle, the development of pore pressure was lower and slower. The specimen did not liquefy in 100 cycles of loading indicating large liquefaction resistance. Specimen S11 with similar fines content, however, non-plastic attained liquefaction ($r_u > 0.95$) in 40 cycles under CSS conditions. The results from the CSS tests on Kutch soils are summarized in Table 4. Maximum shear stress (τ_{\max}) and pore pressure water ratio during the 1st and the 5th cycle are shown. It is evident from the data that the mobilization of shear stresses and development of pore pressure varies over a wide range and is controlled by the FC in silty-sands and PI in clayey-sands. Silty-sand specimens did attain the state of liquefaction whereas clayey-sand specimens did not reach liquefaction in 100 cycles. However, the clayey-sand specimens showed cyclic degradation the magnitude of which was controlled by the PI. At the end of the 5th cycle, the r_u value was found to be higher than 0.62 for all the soils signifying large reduction in the effective confining pressure. The reduced confinement resulted in lower mobilized cyclic strength which was evident from the stress-strain response (Figs. 10 and 12).

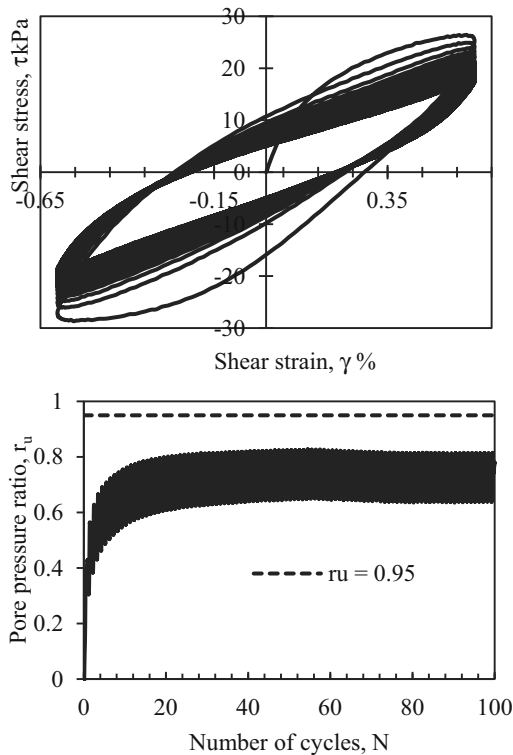


Fig. 12. Behavior of typical clayey-sand (S19) under CSS conditions. (a) Stress-strain and (b) Excess pore water pressure

Table 4. Summary of CSS tests

Soil name	FC	C	Parameters at the end of				Number of cycles to liquefaction
			1 st Cycle		5 th Cycle		
	(%)	(%)	τ_{\max} (kPa)	r_u	τ_{\max} (kPa)	r_u	N_L
<i>Chang Dam</i>							
S2	18	3	15.6	0.91	1.0	0.99	2
S3	19	2	20.1	0.87	2.0	0.98	3
<i>Kharoi</i>							
S4	18	5	18.4	0.81	6.0	0.93	7
S5	11	2	18.3	0.81	5.0	0.95	5
S6	13	2	15.3	0.87	1.1	0.97	3
<i>Suvai Dam</i>							
S7	28	7	16.3	0.85	4.1	0.97	3
S8	24	5	15.2	0.84	2.8	0.95	5
S9	17	3	14.0	0.88	1.7	0.96	4
<i>Fatehgarh Dam</i>							
S11	45	3	22.5	0.62	13.9	0.84	40
S12	22	1	18.4	0.87	3.8	0.98	2
<i>Chobari</i>							
S13	44	2	30.5	0.61	23.7	0.77	>100
S14	49	7	26.5	0.16	16.4	0.76	>100
S15	41	4	23.2	0.35	12.0	0.85	>100
<i>Khadir</i>							
S16	19	2	17.0	0.71	4.5	0.94	10
S17	25	3	17.7	0.76	4.6	0.93	20
S18	10	1	15.6	0.75	2.6	0.95	5
<i>Tappar Dam</i>							
S19	42	18	26.4	0.43	22.5	0.69	>100
S20	29	15	21.6	0.41	18.0	0.62	>100
S21	24	10	21.6	0.37	17.6	0.57	>100
<i>Budharmora</i>							
S22	29	8	20.2	0.78	7.4	0.94	6
<i>Banniari</i>							
S26	83	2	18.4	0.75	4.8	0.96	5

(continued)

Table 4. (continued)

Soil name	FC	C	Parameters at the end of				Number of cycles to liquefaction
			1 st Cycle		5 th Cycle		
	(%)	(%)	τ_{\max} (kPa)	r_u	τ_{\max} (kPa)	r_u	N_L
S27	32	6	19.9	0.79	6.4	0.93	6
S28	21	8	18.0	0.79	8.5	0.95	5
<i>Shivlakra Dam</i>							
S29	29	4	18.0	0.79	4.4	0.95	5
S30	11	2	19.2	0.88	3.1	0.99	2
S31	25	7	19.9	0.81	6.1	0.95	5

3.4 Discussion

The experimental results presented in Sects. 3.1, 3.2 and 3.3 reveal that the monotonic and cyclic strength under undrained conditions of Kutch soils is controlled by the amount and nature of fines. The response of the silty-sands at in-situ density resembled that of static and cyclic liquefaction. The observations from CIUC triaxial tests revealed intense strain softening (static liquefaction) in silty-sands as a common feature, intensity of which was controlled by the fines content (Table 2). As the nature of the fines changes from non-plastic (silty-sands) to plastic (clayey-sands), the response changes from intense strain softening strain hardening. However, for clayey-sands it is not the fines content rather the plasticity index of the fines that governs the behavior. The mechanism governing the effect of plastic and non-plastic fines at particle level can be found elsewhere [19]. The behavior of typical silty-sand from the Kutch under drained, undrained and mix-drained conditions can be found elsewhere [20]. The authors have discussed the effect of stress-ratio on the mix-drained behavior of a typical silty-sand.

Under cyclic conditions, both CTX and CSS, observations regarding the general behavior of Kutch soils were similar as that under CIUC conditions. However, the cyclic resistance of the soils under CSS was observed to lower as compared to CTX conditions. The nature of loading under the two conditions is quite different with CSS conditions more closely simulating the earthquake loading. The magnitude and rate of pore pressure development was higher and faster respectively under CSS conditions. This could be attributed to the nature of the cyclic loading and the mean effective confining pressure. The value of mean effective confining pressure at the start of the test for CTX and CSS is 100 kPa and 67 kPa (assuming at rest conditions with $K_0 = 0.5$). The lower value of p'_i leads to reduced cyclic strength under CSS conditions.

4 Conclusions

Deformation controlled triaxial (CIUC), cyclic triaxial (CTX), and cyclic simple shear (CSS) tests were performed on 31 soil samples from Kutch region at in-situ density. The

results were analyzed in the context of shear strength and excess pore water pressure response. Following conclusions could be drawn from the study:

1. Soil response under the conditions is controlled by both fines content as well as nature of fines. While fines content dominates cohesionless soil behavior, plasticity index dominates the cohesive soil behavior.
2. Silty-sands of Kutch region have inherent tendency to liquefy under static as well as cyclic conditions. This could be attributed to many factors including lower density.
3. Kutch soils showed lower cyclic resistance under CSS conditions. Thus, CTX overestimates the liquefaction resistance and needs a careful evaluation

References

1. Wood, D.M.: Soil Behaviour and Critical State Soil Mechanics. Cambridge University Press, Cambridge (1990)
2. Mitchell, J.K., Soga, K.: Fundamentals of Soil Behavior, vol. 3. Wiley, New York (2005)
3. Schimming, B.B., Haas, H.J., Saxe, H.C.: Study of dynamic and static failure envelopes. *J. Soil Mech. Found. Div.* **92**(2), 105–124 (1966)
4. Ibsen, L.B.: The Static and Dynamic Strength of Sand. Aalborg Univ. (1995)
5. Inci, G., Yesiller, N., Kagawa, T.: Experimental investigation of dynamic response of compacted clayey soils. *Geotech. Test. J.* **26**(2), 125–141 (2003)
6. Yamamuro, J.A., Abrantes, A.E., Lade, P.V.: Effect of strain rate on the stress-strain behavior of sand. *J. Geotech. Geoenviron. Eng.* **137**(12), 1169–1178 (2011)
7. Ishihara, K., Sodekawa, M., Tanaka, Y.: Effects of overconsolidation on liquefaction characteristics of sands containing fines. In: *Dynamic Geotechnical Testing*, pp. 246–264. ASTM, West Conshohocken, PA (1978)
8. Ishihara, K., Takatsu, H.: Effects of overconsolidation and K_0 conditions on the liquefaction characteristics of sands. *Soils Found.* **19**(4), 59–68 (1979)
9. Tatsuoka, F., et al.: Some factors affecting cyclic undrained triaxial strength of sand. *Soils Found.* **26**(3), 99–116 (1986)
10. Tatsuoka, F., Kato, H., Kimura, M., Pradhan, T.B.: Liquefaction strength of sands subjected to sustained pressure. *Soils Found.* **28**(1), 119–131 (1988)
11. Ishihara, K.: *Soil Behavior in Earthquake Geotechnics*. The Oxford Engineering Science Series, No. 46, Oxford, England (1996)
12. Kramer, S.L.: *Geotechnical Earthquake Engineering*. Prentice–Hall International Series in Civil Engineering and Engineering Mechanics. Prentice–Hall, New Jersey (1996)
13. Jefferies, M., Been, K.: *Soil Liquefaction: A Critical State Approach*. CRC Press, Boca Raton (2019)
14. Baki, M.A., Rahman, M.M., Lo, S.R., Gnanendran, C.T.: Linkage between static and cyclic liquefaction of loose sand with a range of fines contents. *Can. Geotech. J.* **49**(8), 891–906 (2012)
15. Hussain, M., Sachan, A.: Post-liquefaction reconsolidation and undrained cyclic behaviour of Chang Dam soil. In: Prashant, A., Sachan, A., Desai, C.S. (eds.) *Advances in Computer Methods and Geomechanics*. LNCE, vol. 55, pp. 77–90. Springer, Singapore (2020). https://doi.org/10.1007/978-981-15-0886-8_7
16. Hussain, M., Sachan, A.: Static liquefaction and effective stress path response of Kutch soils. *Soils Found.* **59**(6), 2036–2055 (2019)

17. Hussain, M., Sachan, A.: Dynamic characteristics of natural Kutch sandy soils. *Soil Dyn. Earthq. Eng.* **125**, 105717 (2019)
18. Hussain, M., Sachan, A.: Cyclic simple shear behaviour of saturated and moist sandy soils. *Geomech. Geoeng.*, 1–24 (2021). <https://doi.org/10.1080/17486025.2021.1975045>
19. Hussain, M., Sachan, A.: Dynamic behaviour of Kutch soils under cyclic triaxial and cyclic simple shear testing conditions. *Int. J. Geotech. Eng.* **14**(8), 902–918 (2020). <https://doi.org/10.1080/19386362.2019.1608715>
20. Gujrati, S., Hussain, M., Sachan, A.: Liquefaction susceptibility of cohesionless soils under monotonic compression and cyclic simple shear loading at drained/undrained/partially drained modes. *Transp. Infrastruct. Geotechnol.*, 1–33 (2022). <https://doi.org/10.1007/s40515-022-00226-6>